

Dynamic analysis of concrete beams reinforced with TiO₂ nano particles under earthquake load

Morteza Sharifi, Reza Kolahchi* and Mahmood Rabani Bidgoli

Department of Civil Engineering, Jasb Branch, Islamic Azad University, Jasb, Iran

(Received August 19, 2017, Revised December 20, 2017, Accepted December 27, 2017)

Abstract. This research studies the dynamic analysis of a concrete column reinforced with titanium dioxide (TiO₂) nanoparticles under earthquake load. The effect of nanoparticles accumulation in a region of concrete column is examined using Mori-Tanaka model. The structure is simulated mathematically based on the theory of sinusoidal shear deformation theory (SSDT). By calculating strain-displacement and stress-strain relations, the system energies include potential energy, kinetic energy, and external works are derived. Then, using the Hamilton's principle, the governing equations for the structure are extracted. Using these equations, the response of the concrete column under earthquake load is investigated using the numerical methods of differential quadrature (DQ) and Newark. The purpose of this study is to study the effects of percentage of nanoparticles, nanoparticles agglomeration, geometric parameters and boundary conditions on the dynamic response of the structure. The results indicate that by increasing the volume percent of TiO₂ nanoparticles, the maximum dynamic deflection of the structure decreases.

Keywords: seismic response; concrete column; TiO₂ nanoparticles; DQ; Newmark method

1. Introduction

So far, a lot of empirical research has been done to model various structures. These modeling are divided into two categories: atomic modeling and continuous environmental mechanistic modeling. The most important techniques for atomic modeling are molecular dynamics, solid bond molecular dynamics and basic density theory. These modeling are highly time consuming and have complex calculations for systems containing many atoms, and, moreover, practical applications of this modeling are very limited. On the other hand, with the advancement of continuous mechanics, it is possible to overcome the limitations of atomic modeling. Today, continuous mechanical models are widely used to model structures. A comparison of the results of atomic modeling and continuous environment mechanics indicates that continuous mechanical modeling has acceptable results in predicting the dynamic behavior of systems. Therefore, most researchers use continuous mechanical modeling to study the dynamic and static behavior of different structures, referred to in the later paragraphs.

In recent years, theoretical and laboratory studies on nanocomposites have been carried out. In this context, Wuite and Adali (2005) performed a stress-strain analysis of reinforced carbon nanotubes. They concluded that the presence of carbon nanotubes as a booster phase can increase the stability and rigidity of the system. Matsuna (2007) examined the stability of composite cylindrical shells with the help of third-order shear theory. Formica

(2010) studied the vibrations of reinforced carbon nanotubes sheets and used the Mori-Tanaka model to match the composite-equivalent properties. Liew *et al.* (2014) analyzed buckling nanocomposite layers. In this study, the mixing rule was used to obtain the equivalent properties of nanocomposites. A non-mesh method was also used to analyze and calculate the buckling load of a nanosized composite structure. In another similar work, Lei *et al.* (2014) analyzed the dynamic stability of panels reinforced with carbon nanotubes. They used the Mori-Tanaka model to simulate nanocomposite properties and obtained the system instability with the help of Ritz's method. The buckling analysis of polymer plates reinforced with carbon nanotubes was carried out by Kolahchi *et al.* (2013). In this work, the mixing rule was used to compute the equivalent properties of the composite. They used the square difference method to obtain the buckling load of the structure. In another work by Kolahchi *et al.* (2016), the dynamic buckling of reinforced carbon nanotube plates was investigated in a functionalized form. The plate properties were considered as temperature dependent and the elastic environment surrounding the structure was simulated using the orthotropic Pasternak model.

In the field of mathematical modeling of concrete structures, very limited work has been done. As a buckling example, reinforced concrete columns reinforced with carbon nanoparticles polymerized by Zamanian *et al.* (2017) along with Safari Bilouei *et al.* (2017). Jafarian Arani *et al.* (2016) studied buckling of reinforced concrete columns with carbon nanotubes, concluding that an increase in the volume of nanotubes resulted in increased buckling load. Analysis of the stresses of concrete pipes reinforced with iron oxide nanoparticles reinforced by iron oxide nanoparticles by Heidarzadeh *et al.* (2017). Arbabi *et al.* (2017) analyzed the buckling of reinforced concrete beams

*Corresponding author, Professor
E-mail: r.kolahchi@gmail.com

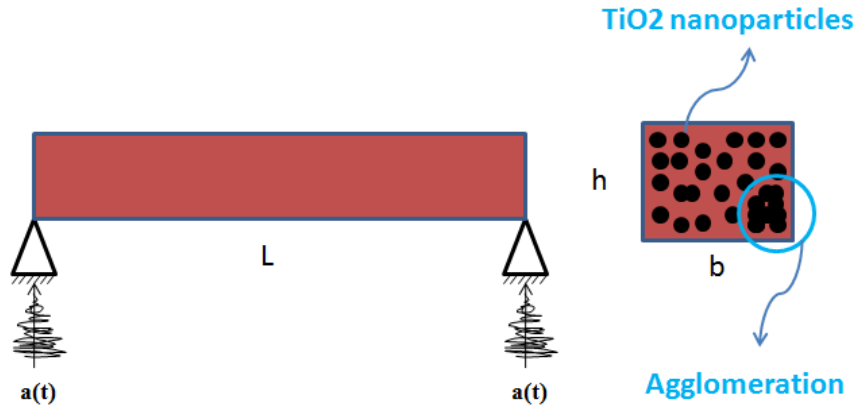


Fig. 1 Concrete column reinforced with titanium dioxide nanoparticles under earthquake load

reinforced with zinc oxide nanoparticles under the electric field.

According to the search of scientific databases in the world, no scholar has investigated the effect of titanium dioxide nanoparticles on the seismic response of concrete beams. This topic is important in the specialty engineering and nanocomposites. Therefore, in this project, the dynamical response of concrete columns reinforced with titanium dioxide nanoparticles under earthquake load is investigated. With the help of the Mori-Tanaka model, the properties of the concrete are equilibrated and the nanoparticles agglomerations are considered. The motion equations are based on the volume percentage of TiO_2 nanoparticles, which can change the effect of nanotechnology on the seismic response. The structure is also mathematically modeled using SSDT and the DQ numerical method is used to obtain the dynamic deflection of the structure.

2. Motion equations

2.1 Stress and strain relations

Fig. 1 shows a concrete column with the length of L , thickness of h and width of b . This column has been reinforced with TiO_2 nanoparticles considering agglomeration effects.

Using the theory of sine wave shear displacement field is as follows (Thai and Vo 2012)

$$u_1(x, z, t) = u(x, t) - z \frac{\partial w(x, t)}{\partial x} + f \psi(x, t), \quad (1)$$

$$u_2(x, z, t) = 0, \quad (2)$$

$$u_3(x, z, t) = w(x, t), \quad (3)$$

where u and w are displacements at the middle plane in the longitudinal and transverse directions, respectively. Also

$$f = \frac{h}{\pi} \sin\left(\frac{\pi z}{h}\right), \quad \psi \text{ also indicates the rotation of the}$$

cross section around the y axis.

Using Eqs. (1)-(3), the strain-displacement equations are written as follows

$$\varepsilon_{xx} = \frac{\partial u}{\partial x} - z \frac{\partial^2 w}{\partial x^2} + f \frac{\partial \psi}{\partial x}, \quad (4)$$

$$\varepsilon_{xz} = \cos\left(\frac{\pi z}{h}\right) \psi, \quad (5)$$

The stress-strain relations of the structure are simplified as follows

$$\sigma_{xx} = C_{11} \varepsilon_{xx}, \quad (6)$$

$$\sigma_{xz} = C_{55} \gamma_{xz}, \quad (7)$$

2.2 Mori-Tanaka model

In this section, the properties and coefficients of concrete beam reinforced with TiO_2 nanoparticles are examined from a micro-mechanical viewpoint. It is assumed that the concrete beam is isotropic, and the Young modulus and its Poisson ratio coefficient are E_m and ν_m respectively. The stress-strain relation in the local coordinates of an elementary element in this case is expressed as follows (Mori and Tanaka 1973)

$$\begin{Bmatrix} \sigma_{11} \\ \sigma_{22} \\ \sigma_{33} \\ \sigma_{23} \\ \sigma_{13} \\ \sigma_{12} \end{Bmatrix} = \begin{bmatrix} k+m & l & k-m & 0 & 0 & 0 \\ l & n & l & 0 & 0 & 0 \\ k-m & l & k+m & 0 & 0 & 0 \\ 0 & 0 & 0 & p & 0 & 0 \\ 0 & 0 & 0 & 0 & m & 0 \\ 0 & 0 & 0 & 0 & 0 & p \end{bmatrix} \begin{Bmatrix} \varepsilon_{11} \\ \varepsilon_{22} \\ \varepsilon_{33} \\ \gamma_{23} \\ \gamma_{13} \\ \gamma_{12} \end{Bmatrix} \quad (8)$$

In the above equation, k, l, m, n, p are elastic modulus of Hill which are

$$\begin{aligned} k &= \frac{E_m \{E_m c_m + 2k_r(1+\nu_m)[1+c_r(1-2\nu_m)]\}}{2(1+\nu_m)[E_m(1+c_r-2\nu_m) + 2c_m k_r(1-\nu_m-2\nu_m^2)]} \\ l &= \frac{E_m \{c_m \nu_m [E_m + 2k_r(1+\nu_m)] + 2c_r l_r(1-\nu_m^2)\}}{(1+\nu_m)[E_m(1+c_r-2\nu_m) + 2c_m k_r(1-\nu_m-2\nu_m^2)]} \\ n &= \frac{E_m^2 c_m(1+c_r-c_m \nu_m) + 2c_m c_r(k_r n_r - l_r^2)(1+\nu_m)^2(1-2\nu_m)}{(1+\nu_m)[E_m(1+c_r-2\nu_m) + 2c_m k_r(1-\nu_m-2\nu_m^2)]} \\ &\quad + \frac{E_m[2c_m^2 k_r(1-\nu_m) + c_r n_r(1+c_r-2\nu_m) - 4c_m l_r \nu_m]}{E_m(1+c_r-2\nu_m) + 2c_m k_r(1-\nu_m-2\nu_m^2)} \quad (9) \\ p &= \frac{E_m[E_m c_m + 2p_r(1+\nu_m)(1+c_r)]}{2(1+\nu_m)[E_m(1+c_r) + 2c_m p_r(1+\nu_m)]} \\ m &= \frac{E_m[E_m c_m + 2m_r(1+\nu_m)(3+c_r-4\nu_m)]}{2(1+\nu_m)\{E_m[c_m + 4c_r(1-\nu_m)] + 2c_m m_r(3-\nu_m-4\nu_m^2)\}} \end{aligned}$$

In the above relations k_r, l_r, n_r, p_r, m_r are the elasticity modulus of the Hill for the reinforced phase (TiO_2 nanoparticles). Experimental results show that most nanoparticles are irregular (Shi and Feng 2004). A large amount of nanoparticles inside the composite are concentrated in a region (Shi and Feng 2004). This region is supposed to be spherical and we call it the so-called "space" which has different properties with the surrounding material. V_r is the final volume of nanoparticles and we will have

$$V_r = V_r^{inclusion} + V_r^m \quad (10)$$

In which $V_r^{inclusion}$ and V_r^m are the volume of nanoparticles in the capacity and the concrete, respectively. The following two parameters are used to show the agglomeration effect in a micromechanical model

$$\xi = \frac{V_{inclusion}}{V}, \quad (11)$$

$$\zeta = \frac{V_r^{inclusion}}{V_r}. \quad (12)$$

C_r is the volume fraction of the nanoparticles in the concrete beam as follows

$$C_r = \frac{V_r}{V}. \quad (13)$$

Assuming that the isotropic nanoparticles are transverse and are completely randomly located in the capacity, the isotropic capacity is assumed, and using the Mori-Tanaka method for the isotropic materials, the volume modulus K and the shear modulus G are as follows

$$K = K_{out} \left[1 + \frac{\xi \left(\frac{K_{in}}{K_{out}} - 1 \right)}{1 + \alpha(1-\xi) \left(\frac{K_{in}}{K_{out}} - 1 \right)} \right], \quad (14)$$

$$G = G_{out} \left[1 + \frac{\xi \left(\frac{G_{in}}{G_{out}} - 1 \right)}{1 + \beta(1-\xi) \left(\frac{G_{in}}{G_{out}} - 1 \right)} \right], \quad (15)$$

In the above relations, K_{in} and K_{out} , respectively, have a volumetric capacitance and composite capacity minus, respectively, and G_{in} and G_{out} respectively have a volumetric capacitance and composite capacity minus, respectively, obtained from the following relationships

$$K_{in} = K_m + \frac{(\delta_r - 3K_m \chi_r) C_r \zeta}{3(\xi - C_r \zeta + C_r \zeta \chi_r)}, \quad (16)$$

$$K_{out} = K_m + \frac{C_r(\delta_r - 3K_m \chi_r)(1-\zeta)}{3[1-\xi - C_r(1-\zeta) + C_r \chi_r(1-\zeta)]}, \quad (17)$$

$$G_{in} = G_m + \frac{(\eta_r - 3G_m \beta_r) C_r \zeta}{2(\xi - C_r \zeta + C_r \zeta \beta_r)}, \quad (18)$$

$$G_{out} = G_m + \frac{C_r(\eta_r - 3G_m \beta_r)(1-\zeta)}{2[1-\xi - C_r(1-\zeta) + C_r \beta_r(1-\zeta)]}, \quad (19)$$

where $\chi_r, \beta_r, \delta_r, \eta_r$ are

$$\chi_r = \frac{3(K_m + G_m) + k_r - l_r}{3(k_r + G_m)}, \quad (20)$$

$$\beta_r = \frac{1}{5} \left\{ \frac{4G_m + 2k_r + l_r}{3(k_r + G_m)} + \frac{4G_m}{(p_r + G_m)} + \frac{2[G_m(3K_m + G_m) + G_m(3K_m + 7G_m)]}{G_m(3K_m + G_m) + m_r(3K_m + 7G_m)} \right\}, \quad (21)$$

$$\delta_r = \frac{1}{3} \left[n_r + 2l_r + \frac{(2k_r - l_r)(3K_m + 2G_m - l_r)}{k_r + G_m} \right], \quad (22)$$

$$\eta_r = \frac{1}{5} \left[\frac{2}{3}(n_r - l_r) + \frac{4G_m p_r}{(p_r + G_m)} + \frac{8G_m m_r(3K_m + 4G_m)}{3K_m(m_r + G_m) + G_m(7m_r + G_m)} + \frac{2(k_r - l_r)(2G_m + l_r)}{3(k_r + G_m)} \right]. \quad (23)$$

Also, K_m and G_m are the volumetric and shear modulus of the base phase, respectively which are

$$K_m = \frac{E_m}{3(1-2\nu_m)}, \quad (24)$$

$$G_m = \frac{E_m}{2(1+\nu_m)}. \quad (25)$$

In addition β, α , are

$$\alpha = \frac{(1 + \nu_{out})}{3(1 - \nu_{out})}, \quad (26)$$

$$\beta = \frac{2(4 - 5\nu_{out})}{15(1 - \nu_{out})}, \quad (27)$$

$$\nu_{out} = \frac{3K_{out} - 2G_{out}}{6K_{out} + 2G_{out}}. \quad (28)$$

By obtaining the K modulus and the shear modulus G of the nanocomposite using the above relations, E and ν are obtained from the following equation

$$E = \frac{9KG}{3K + G}, \quad (29)$$

$$\nu = \frac{3K - 2G}{6K + 2G}. \quad (30)$$

2.3 Energy method

One of the most comprehensive ways to get the governing equations of the system is to write energy and apply the principle of Hamilton. The potential energy of the structure is given by

$$U = \frac{1}{2} \int_V (\sigma_{xx} \varepsilon_{xx} + \sigma_{xz} \gamma_{xz}) dV, \quad (31)$$

By substituting Eqs. (4) and (5) into Eq. (31), the potential energy is as follows:

$$U = \frac{1}{2} \int_V \left(\sigma_{xx} \left(\frac{\partial u}{\partial x} - z \frac{\partial^2 w}{\partial x^2} + f \frac{\partial \psi}{\partial x} \right) + \sigma_{xz} \left(\cos\left(\frac{\pi z}{h}\right) \psi \right) \right) dV, \quad (32)$$

By defining the forces and moments resultants in the page as follows

$$(N_x, M_x, P_x) = \int_A (1, z, f) \sigma_x dA, \quad (33)$$

$$Q_x = \int_A \cos\left(\frac{\pi z}{h}\right) \sigma_{xz} dA, \quad (34)$$

the potential energy can be simplified as follows

$$U = \int_x \left(N_x \frac{\partial u}{\partial x} - M_x \frac{\partial^2 w}{\partial x^2} + P_x \frac{\partial \psi}{\partial x} + Q_x \psi \right) dx. \quad (35)$$

The Kinetic energy is written in the general form as follows

$$K = \frac{\rho}{2} \int_V \left(\left(\frac{\partial u_1}{\partial t} \right)^2 + \left(\frac{\partial u_2}{\partial t} \right)^2 + \left(\frac{\partial u_3}{\partial t} \right)^2 \right) dV, \quad (36)$$

where ρ is the density of the structure. Substituting Eqs. (1)-(3) in the above relation yields

$$K = \int \left[I_0 \left(\frac{\partial u}{\partial t} \right)^2 + \left(\frac{\partial w}{\partial t} \right)^2 + I_2 \left(\frac{\partial^2 w}{\partial x \partial t} \right)^2 - \frac{24}{\pi^3} \frac{\partial w}{\partial x} \frac{\partial \psi}{\partial t} - \frac{24}{\pi^3} \frac{\partial w}{\partial t} \frac{\partial \psi}{\partial x} + \frac{6}{\pi^2} \left(\frac{\partial \psi}{\partial t} \right)^2 \right] dx. \quad (37)$$

The external work of earthquake forces is as follows

$$W = \int F_{Seismic} (ma(t)) w dA, \quad (38)$$

where m and $a(t)$ are the mass and acceleration of the earth, respectively. Hamilton's principle is expressed as follows

$$\int_0^t (\delta U - \delta K - \delta W) dt = 0, \quad (39)$$

By inserting Eqs. (35), (37) and (38) into Eq. (39) and using the integral of the component and arranging the relations in the direction of mechanical displacement, the three motion equations are as follows

$$\delta u : \frac{\partial N_x}{\partial x} = I_0 \frac{\partial^2 u}{\partial t^2}. \quad (40)$$

$$\delta w : \frac{\partial^2 M_x}{\partial x^2} = I_0 \frac{\partial^2 w}{\partial t^2} + \frac{24I_2}{\pi^3} \frac{\partial^2 \psi}{\partial x \partial t} - I_2 \frac{\partial^4 w}{\partial x^2 \partial t^2} + F_{Seismic}. \quad (41)$$

$$\delta \psi : \frac{\partial P_x}{\partial x} - Q_x = \frac{6I_2}{\pi^2} \frac{\partial^2 \psi}{\partial t^2} - \frac{24I_2}{\pi^3} \frac{\partial^2 w}{\partial x \partial t}. \quad (42)$$

By inserting Eqs. (4)-(7) into Eqs. (33) and (34), the internal forces and moments of the column can be calculated as follows

$$N_x = hC_{11} \frac{\partial u}{\partial x}, \quad (43)$$

$$M_x = -C_{11}I \frac{\partial^2 w}{\partial x^2} + \frac{24C_{11}I}{\pi^3} \frac{\partial \psi}{\partial x}, \quad (44)$$

$$P_x = -\frac{24C_{11}I}{\pi^3} \frac{\partial^2 w}{\partial x^2} + \frac{6C_{11}I}{\pi^2} \frac{\partial \psi}{\partial x}, \quad (45)$$

$$Q_x = \frac{C_{55}A}{2} \psi, \quad (46)$$

where

$$(A, I) = \int_A (1, z^2) dA, \quad (47)$$

Now, with substituting Eqs. (43) to (46) into Eqs. (40) to (42), the relations are obtained in terms of mechanical displacements as

$$\delta u : \frac{\partial^2 u}{\partial x^2} = I_0 \frac{\partial^2 u}{\partial t^2}, \quad (48)$$

$$\delta w : -Q_{11} I \frac{\partial^4 w}{\partial x^4} + \frac{24Q_{11} I}{\pi^3} \frac{\partial^3 \psi}{\partial x^3} = I_0 \frac{\partial^2 w}{\partial t^2} + \frac{24I_2}{\pi^3} \frac{\partial^2 \psi}{\partial x \partial t} - I_2 \frac{\partial^4 w}{\partial x^2 \partial t^2} + F_{Seismic}, \quad (49)$$

$$\delta \psi : -\frac{24Q_{11} I}{\pi^3} \frac{\partial^3 w}{\partial x^3} + \frac{6Q_{11} I}{\pi^2} \frac{\partial^2 \psi}{\partial x^2} - \frac{Q_{55} A}{2} \psi = \frac{6I_2}{\pi^2} \frac{\partial^2 \psi}{\partial t^2} - \frac{24I_2}{\pi^3} \frac{\partial^2 w}{\partial x \partial t}, \quad (50)$$

The boundary conditions in this project are considered as follows

❖ Clamped- Clamped

$$w = u = \frac{\partial w}{\partial x} = 0 \quad @ \quad x = 0, L \quad (51)$$

❖ Simply- Simply

$$u = w = \frac{\partial^2 w}{\partial x^2} = 0 \quad @ \quad x = 0, L \quad (52)$$

❖ Clamped-Simply

$$\begin{aligned} w = u = \frac{\partial w}{\partial x} = 0 & \quad @ \quad x = 0 \\ u = w = \frac{\partial^2 w}{\partial x^2} = 0 & \quad @ \quad x = L \end{aligned} \quad (53)$$

3. Numerical method

3.1 DQ method

The DQ method is one of the numerical methods in which the weighting coefficients of the governing differential equations are converted into a set of first-order algebraic equations. In this way, at each point, the derivative is expressed as a linear sum of the weight coefficients and the function values at that point and other points of the domain in the direction of the coordinate axes. The main relation of these methods for a one-dimensional state is expressed as follows (Kolahchi *et al.* 2016)

$$\frac{df}{dx} \Big|_{x=x_i} \rightarrow = \sum_{j=1}^N C_{ij} f_j \quad (54)$$

where $f(x)$ is desired function, N is number of sample points and C_{ij} is the weighting coefficients to obtain the

derivative of the function at the sample point. Chebyshev's polynomial roots are used to solve engineering problems and bring good results. This transition distance is expressed as follows

$$X_i = \frac{L}{2} \left[1 - \cos \left(\frac{i-1}{N_x-1} \pi \right) \right] \quad i = 1, \dots, N_x \quad (55)$$

The weighting coefficients are

$$C_{ij}^{(1)} = \frac{L_1(x_i)}{(x_i - x_j) L_1(x_j)} \quad \text{for } i \neq j, \quad i, j = 1, 2, \dots, N \quad (56)$$

$$C_{ii}^{(1)} = - \sum_{j=1, j \neq i}^N C_{ij}^{(1)} \quad \text{for } i = j, \quad i = 1, 2, \dots, N. \quad (57)$$

According to the above-mentioned relations for solving the governing equations that were calculated in the previous chapter, the structures along the length are divided to N section. As a result, the points relating to the boundary condition and the field must be separated from each other. Consequently, the governing equations and boundary conditions in the matrix form are written as follows

$$\left([K] \begin{Bmatrix} \{d_b\} \\ \{d_d\} \end{Bmatrix} + [C] \begin{Bmatrix} \{\dot{d}_b\} \\ \{\dot{d}_d\} \end{Bmatrix} + [M] \begin{Bmatrix} \{\ddot{d}_b\} \\ \{\ddot{d}_d\} \end{Bmatrix} \right) = \begin{Bmatrix} \{0\} \\ -Ma(t) \end{Bmatrix}, \quad (58)$$

In the above $[K]$, $[C]$ and $[M]$ are respectively, the matrix of stiffness, the matrix of the damp and the matrix of the mass. Also, in the order of the dynamic range vector, the boundary condition $\{d_b\}$ and $\{d_d\}$ field conditions are considered.

3.2 Newmark method

In this section, Newmark's numerical method (Simsek, 2010) has been used in the time domain to obtain the time response of a structure under earthquake load. Based on this method, Eq. (58) is written in the following general form

$$K^*(d_{i+1}) = Q_{i+1}, \quad (59)$$

where the $i + 1$ subtitle indicates time ($t = ti + 1$), $K^*(d_{i+1})$ is the effective matrix and Q_{i+1} is the effective force vector which are written as follows

$$K^*(d_{i+1}) = K_L + K_{NL}(d_{i+1}) + \alpha_0 M + \alpha_1 C, \quad (60)$$

$$Q_{i+1}^* = Q_{i+1} + M(\alpha_0 d_i + \alpha_2 \dot{d}_i + \alpha_3 \ddot{d}_i) + C(\alpha_1 d_i + \alpha_4 \dot{d}_i + \alpha_5 \ddot{d}_i), \quad (61)$$

where (Simsek 2010)

$$\begin{aligned} \alpha_0 &= \frac{1}{\chi \Delta t^2}, & \alpha_1 &= \frac{\gamma}{\chi \Delta t}, & \alpha_2 &= \frac{1}{\chi \Delta t}, & \alpha_3 &= \frac{1}{2\chi} - 1, & \alpha_4 &= \frac{\gamma}{\chi} - 1, \\ \alpha_5 &= \frac{\Delta t}{2} \left(\frac{\gamma}{\chi} - 2 \right), & \alpha_6 &= \Delta t(1 - \gamma), & \alpha_7 &= \Delta t \gamma, \end{aligned} \quad (62)$$

In the above relations $\gamma=0.5$ and $\chi=0.25$. Based on the iterative method, Eq. (59) is solved at each time interval and the acceleration and the modified speed are calculated from the following relationships

$$\ddot{d}_{i+1} = \alpha_0(d_{i+1} - d_i) - \alpha_2\dot{d}_i - \alpha_3\ddot{d}_i, \quad (63)$$

$$\dot{d}_{i+1} = \dot{d}_i + \alpha_6\ddot{d}_i + \alpha_7\ddot{d}_{i+1}, \quad (64)$$

Then, for the next time interval, the acceleration and speed corrected in relations (63) and (64) are used and the mentioned steps should be repeated again.

4. Results and discussion

In this chapter, we examine the numerical results for the dynamic response of concrete column reinforced with titanium dioxide nanoparticles under earthquake load. For this purpose, a concrete column with length $L = 3m$ and thickness $h = 15 cm$, elastic modulus $E_m = 20 GPa$ and Poisson's ratio $\nu_m = 0.3$ is considered, which is strengthened with TiO_2 nanoparticles with elastic modulus $E_r = 160 GPa$ and Poisson's ratio $\nu_r = 0.2$. It should be noted that for the acceleration of the earthquake, the Cape Mendocino region is considered that its acceleration distribution in 30 seconds is shown in Fig. 2.

4.1 Validation of results

Given the fact that this project was first defined globally, there is no reference to measuring the results. Therefore, in this section, we try to examine the linear dynamic response of the structure by two methods and compare the results with each other.

• The first method

In this method, which is found in most references, the response is calculated using vibrational modes. Also, in this section the simply supported boundary condition is used as

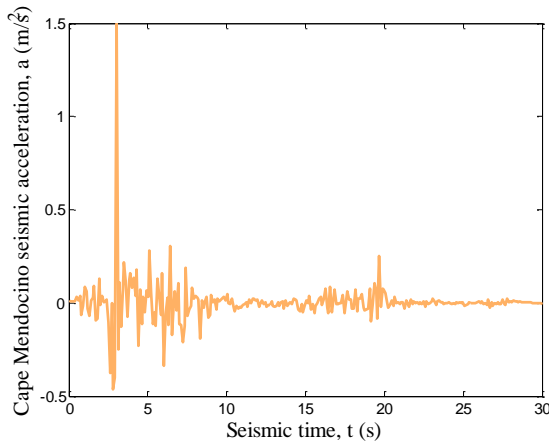


Fig. 2 Acceleration of the Cape Mendocino earthquake

$$d = \begin{Bmatrix} u \\ v \\ \psi \end{Bmatrix} = \begin{Bmatrix} A_1 \cos\left(\frac{m\pi x}{l}\right) \\ A_2 \sin\left(\frac{m\pi x}{l}\right) \\ A_3 \sin\left(\frac{m\pi x}{l}\right) \end{Bmatrix}, \quad (65)$$

In the above relation A_i ($i=1, \dots, 3$) and m respectively, are the dynamic amplitude and the longitudinal half-wave number. By inserting Eq. (65) into linear motion equations and writing them in the form of a matrix, we have

$$([K]\{d\} + [M]\{\ddot{d}\}) = \{-Ma(t)\}, \quad (66)$$

where $[M_{ij}]$ ($i, j = 1, \dots, 3$) and $[K_{ij}]$ ($i, j = 1, \dots, 3$), respectively, are mass and stiffness matrixes. Finally, using the Newmark method, the dynamic response can be obtained.

• The second method

In this method, DQM is used. In this way, the governing equations are derived from the description of Chapters 2 and 3 in the form of Eq. (66) and using the Newmark method, the dynamic response can be calculated.

The results of the analytical method and the DQ numerical method are shown in Fig. 3. It is observed that the error of the DQM numerical method is insignificant and acceptable with respect to the analytical method, which is a sign of the accuracy for the results of this work.

4.2 Numerical method convergence

Fig. 4 shows the convergence of the DQ numerical method on the maximum dynamic deflection of the structure in terms of the number of grid points. As can be seen, with increasing the number of grid points, the maximum dynamic deflection of the structure decreases to the extent that it converges in both positions. Therefore, in the calculations performed in this project, the number of grid points for the DQ method is 13.

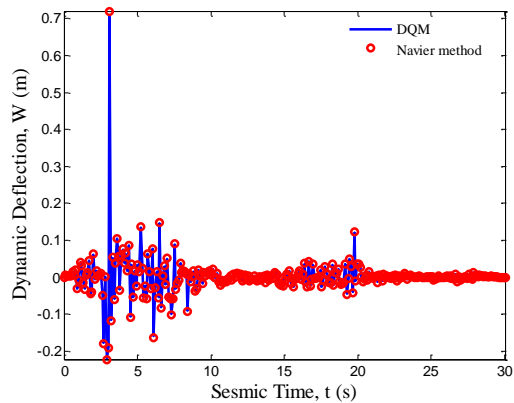


Fig. 3 Comparison of numerical and analytical results

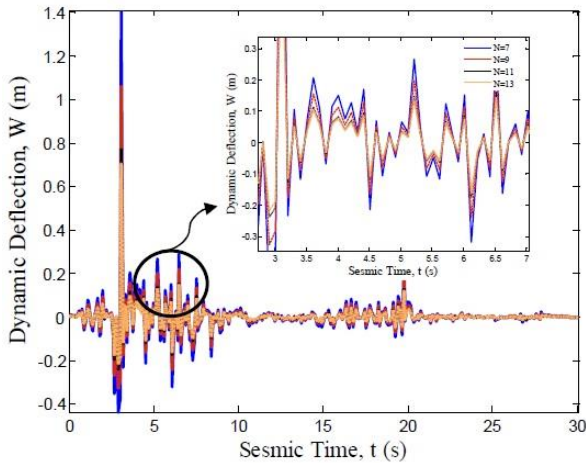


Fig. 4 Convergence of the numerical method

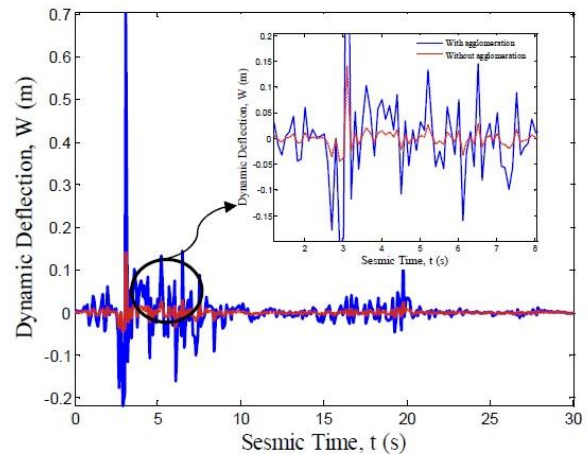


Fig. 6 The effect of TiO₂ nanoparticles agglomeration on the dynamics deflection of the structure

4.3 The effect of different parameters

❖ Effect of TiO₂ nanoparticles

Fig. 5 shows the effect of the volume percentage of the TiO₂ nanoparticles on the dynamic deflection of the structure in terms of time. With regard to the figure, it is clear that the larger the volume percentage of TiO₂ nanoparticles, the dynamic deflection of the system decreases since the structure rigidity rises.

Fig. 6 shows the agglomeration effect of TiO₂ nanoparticles in a particular region on the dynamic deflection of the structure. As can be seen, considering the agglomeration of TiO₂ nanoparticles decreases the stiffness of the structure and increases the displacement. Since in the nano-composite columns, nanoparticles cannot be uniformly distributed, the results of this graph can be very important.

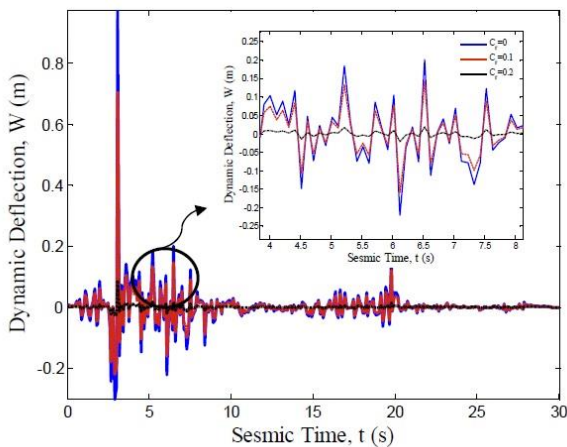


Fig. 5 The effect of volume percent of TiO₂ nanoparticles on the dynamics deflection of the structure

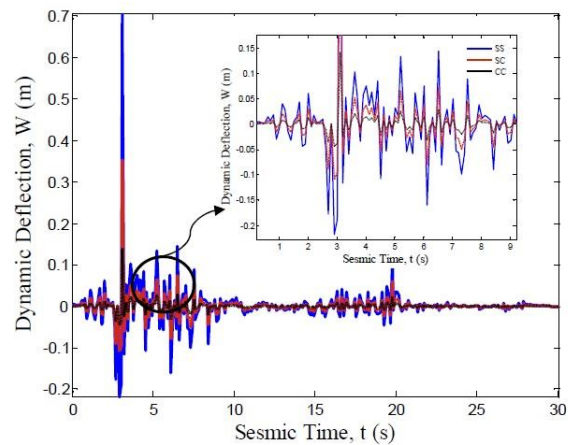


Fig. 7 The effect of boundary conditions on the dynamics deflection of the structure

❖ The effect of boundary conditions

Fig. 7 illustrates the effect of different boundary conditions on dynamic displacement. As it is seen, boundary conditions have a significant effect on the dynamic displacement of the system so that the column with the clamped boundary conditions at the two ends will have a lower dynamic displacement. The reason for this is that the structure is less tight and therefore more rigid. Also, in the boundary conditions, the simple boundary condition has more dynamic displacement.

❖ The effect of geometrical parameters

The effect of the thickness of the column on the dynamic displacement is shown in Fig. 8. It can be seen that as the column thickness increases, the dynamic displacement of the system decreases, due to the rigidity of the structure with increasing thickness. Fig. 9 presents the effect of column length on the dynamic displacement of the

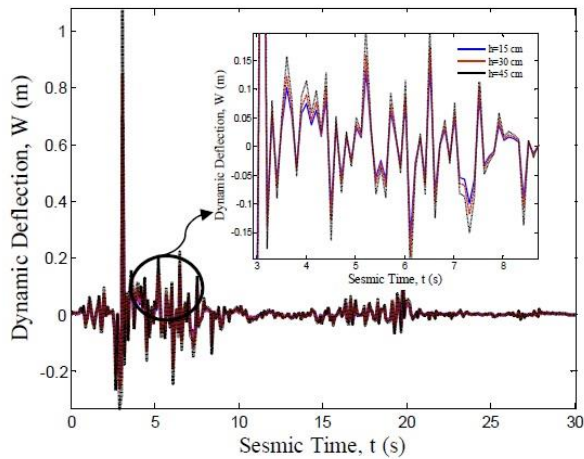


Fig. 8 The effect of column thickness on the dynamics deflection of the structure

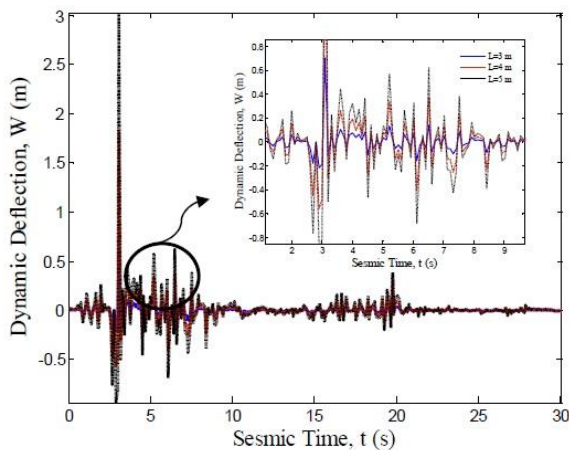


Fig. 9 The effect of column length on the dynamics deflection of the structure

structure in terms of time. The increase in the length leads to an increase in the displacement of the structure. The reason for this is reduce the rigidity of the system by increasing the length of the column.

5. Conclusions

In this research, the dynamic response of a nano-composite concrete column under earthquake load was investigated using the DQ and Newmark methods. The column was reinforced by titanium dioxide nanoparticles which the effective material properties were obtained by Mori-Tanaka model taking into account the agglomeration of nanoparticles. Using nonlinear strain-displacement equations of SSDT, stress-strain relations, the total energy equations are obtained and using Hamilton's method, the motion equations were derived. The purpose of this study was to investigate the effects of the volume percentages of TiO₂ nanoparticles, the agglomeration of TiO₂ nanoparticles, boundary conditions and column geometric parameters on

the dynamic displacement of the structure. According to the graphs drawn, the following results are obtained:

- ❖ The error of the DQ numerical method is negligible in comparison with the analytical method, which is a sign of the accuracy for the results of this work.
- ❖ As the volume percentage of TiO₂ nanoparticles increases, the dynamic deflection of the system decreases.
- ❖ Consideration of the agglomeration of TiO₂ nanoparticles reduces the stiffness of the structure and increases the displacement of the structure.
- ❖ Boundary conditions have a significant effect on the dynamic displacement of the system so that the column with the clamped boundary conditions at the two ends will have a lower dynamic displacement.
- ❖ By increasing the thickness of the column, the dynamic displacement of the system decreases, due to the rigidity of the structure with increasing thickness.
- ❖ The increase in length of column leads to an increase in the displacement of the structure.

References

- Arbabi, A., Kolahchi, R. and Rabani Bidgoli, M. (2017), "Concrete columns reinforced with Zinc Oxide nanoparticles subjected to electric field: buckling analysis", *Wind. Struct.*, **24**(5), 431-446.
- Formica, G., Lacarbonara, W. and Alessi, R. (2010), "Vibrations of carbon nanotube reinforced composites", *J. Sound Vib.*, **329**(10), 1875-1889.
- Jafarian Arani, A. and Kolahchi, R. (2016), "Buckling analysis of embedded concrete columns armed with carbon nanotubes", *Comput. Concrete*, **17**(5), 567-578.
- Heidarzadeh, A., Kolahchi, R. and Rabani Bidgoli, M. (2017), "Concrete pipes reinforced with AL₂O₃Nanoparticles considering agglomeration: magneto-thermo-mechanical stress analysis", *Int. J. Civ. Eng.*, In press.
- Kolahchi, R., Rabani Bidgoli, M., Beygipour, Gh. and Fakhar, M.H. (2013), "A nonlocal nonlinear analysis for buckling in embedded FG-SWCNT-reinforced microplates subjected to magnetic field", *J. Mech. Sci. Tech.*, **5**, 2342-2355.
- Kolahchi, R., Safari, M. and Esmailpour, M. (2016), "Dynamic stability analysis of temperature-dependent functionally graded CNT-reinforced visco-plates resting on orthotropic elastomeric medium", *Compos. Struct.*, **150**, 255-265.
- Lei, Z.X., Zhang, L.W., Liew, K.M. and Yu, J.L. (2014), "Dynamic stability analysis of carbon nanotube-reinforced functionally graded cylindrical panels using the element-free kp-Ritz method", *Compos. Struct.*, **113**, 328-338.
- Liew, K.M., Lei, Z.X., Yu, J.L. and Zhang, L.W. (2014), "Postbuckling of carbon nanotube-reinforced functionally graded cylindrical panels under axial compression using a meshless approach", *Comput. Method. Appl. M.*, **268**, 1-17.
- Matsuna, H. (2007), "Vibration and buckling of cross-ply laminated composite circular cylindrical shells according to a global higher-order theory", *Int. J. Mech. Sci.*, **49**(9), 1060-1075.
- Mori, T. and Tanaka, K. (1973), "Average stress in matrix and average elastic energy of materials with misfitting inclusions", *Acta Metall. Mater.*, **21**(5), 571-574.
- Safari Bilouei, B., Kolahchi, R. and Rabani Bidgoli, M. (2017),

- “Buckling of concrete columns retrofitted with Nano-Fiber Reinforced Polymer (NFRP)”, *Comput. Concrete*, **18**, 1053-1063.
- Shi, D.L. and Feng, X.Q. (2004), “The effect of nanotube waviness and agglomeration on the elastic property of carbon nanotube-reinforced composite”, *J. Eng. Mat. Tech ASME*, **126**(3), 250-270.
- Simsek, M. (2010), “Non-linear vibration analysis of a functionally graded Timoshenko beam under action of a moving harmonic load”, *Compos. Struct.*, **92**(10), 2532-2546.
- Thai, H.T. and Vo, T.P. (2012), “A nonlocal sinusoidal shear deformation beam theory with application to bending, buckling, and vibration of nanobeams”, *Int. J. Eng. Sci.*, **54**, 58-66.
- Wuite, J. and Adali, S. (2005), “Deflection and stress behaviour of nanocomposite reinforced beams using a multiscale analysis”, *Compos. Struct.*, **71**(3-4), 388-396.
- Zamanian, M., Kolahchi, R. and Rabani Bidgoli, M. (2017), “Agglomeration effects on the buckling behaviour of embedded concrete columns reinforced with SiO_2 nano-particles”, *Wind Struct.*, **24**(1), 43-57.

CC

